Journal of Power Sources 195 (2010) 6088–6094

Contents lists available at ScienceDirect

Journal of Power Sources

journal homepage: www.elsevier.com/locate/jpowsour

Preparation and electrochemical characterization of polymer electrolytes based on electrospun poly(vinylidene fluoride-*co*-hexafluoropropylene)/polyacrylonitrile blend/composite membranes for lithium batteries

Prasanth Raghavan[a], Xiaohui Zhao[a], Chorong Shin[a], Dong-Ho Baek[a], Jae-Won Choi[a], James Manuel[a], Min-Yeong Heo[a], Jou-Hyeon Ahn[a,*], Changwoon Nah[b]

[a] Department of Chemical and Biological Engineering and Engineering Research Institute, Gyeongsang National University, 900, Gajwa-dong, Jinju 660-701, Republic of Korea
[b] Department of Polymer-Nano Science and Technology, Chonbuk National University, 664-14, Duckjin-dong, Jeonju 561-756, Republic of Korea

ARTICLE INFO

Article history:
Received 25 September 2009
Received in revised form
21 November 2009
Accepted 24 November 2009
Available online 3 December 2009

Keywords:
Polymer electrolytes
Electrospinning
Blend/composite membranes
Polyacrylonitrile
Poly(vinylidene fluoride-*co*-hexafluoropropylene)

ABSTRACT

Apart from PEO based solid polymer electrolytes, tailor-made gel polymer electrolytes based on blend/composite membranes of poly(vinylidene fluoride-*co*-hexafluoropropylene) and polyacrylonitrile are prepared by electrospinning using 14 wt% polymer solution in dimethylformamide. The membranes show uniform morphology with an average fiber diameter of 320–490 nm, high porosity and electrolyte uptake. Polymer electrolytes are prepared by soaking the electrospun membranes in 1 M lithium hexafluorophosphate in ethylene carbonate/dimethyl carbonate. Temperature dependent ionic conductivity and their electrochemical performance are studied. The blend/composite polymer electrolytes show good ionic conductivity in the range of 10^{-3} S cm^{-1} at ambient temperature and good electrochemical performance. All the Polymer electrolytes show an anodic stability >4.6 V with stable interfacial resistance with storage time. The prototype cell shows good charge–discharge properties and stable cycle performance with comparable capacity fade compared to liquid electrolyte under the test conditions.

1. Introduction

Recently polymer electrolytes (PEs) have received considerable attention for application in rechargeable secondary batteries, fuel cells, supercapacitors, etc., since they can offer systems that are lighter, safer and more flexible in shape compared with their liquid counterparts [1,2]. Many efforts have been done to enhance the electrochemical properties of PEs in order to make them feasible for power applications. Poly(vinylidene fluoride) (PVdF) [3–5] and its copolymer poly(vinylidene fluoride-*co*-hexafluoropropylene) (P(VdF-*co*-HFP)) [1,2,6–9], poly(ethylene glycol) [10], poly(urethane acrylate) [11], polyacrylonitrile (PAN) [12], poly(methyl methacrylate) (PMMA) [13] and poly(ethylene oxide) (PEO) [14] have been widely used as polymer matrices for the preparation of PEs. Among them, P(VdF-*co*-HFP) has been found to be very promising as it has good electrochemical stability, affinity to electrolyte solution and high dielectric constant ($\varepsilon \approx 8.4$). The formation of stable LiF and >C=CF– unsaturated bonds through interactions between the fluorine atoms in PVdF part of the polymer and lithium or lithiated graphite is one of the problems to restrict the use of P(VdF-*co*-HFP) based membranes for polymer electrolyte [15]. It has been reported that PVdF-based membranes are miscible with liquid electrolytes that are generally used for the preparation of PEs [16,17]. Therefore, a multiphase electrolyte consisting of liquid electrolyte and polymer gel electrolyte is often formed when P(VdF-*co*-HFP)-based membrane is used as a separator in lithium batteries. This could result in a loss of mechanical strength and internal short-circuits. Nevertheless, the leakage of electrolyte solution is due to phase separation between the polymer matrix and the absorbed electrolyte solution. The solvent loss may also lead to a failing of the electrode/electrolyte contact as well as a reduction of ionic conductivity. The crystalline part of P(VdF-*co*-HFP) hinders the migration of Li^+ ions and hence batteries with P(VdF-*co*-HFP) based electrolytes have lower charge/discharge capacities and poor *C*-rate values [18]. Therefore, it is of great importance to search for novel polymer electrolytes to create a new generation of high performance lithium batteries. Blending/composite preparation of two or more polymers can be used for bypassing these limitations [19,20].

* Corresponding author. Tel.: +82 55 751 5388; fax: +82 55 753 1806.
E-mail address: jhahn@gnu.ac.kr (J.-H. Ahn).

0378-7753/$ – see front matter © 2009 Elsevier B.V. All rights reserved.
doi:10.1016/j.jpowsour.2009.11.098

It is found that PAN [21] has good processability, flame resistance, resistance to oxidative degradation and electrochemical stability. Oxidative stabilization of PAN is very high even at high temperature. PAN-based electrolyte has shown interesting characteristics like high ionic conductivity, thermal stability, good morphology for electrolyte uptake and compatibility with lithium electrode. Tsutsumi et al. [22] reported that PAN-based polymer electrolytes minimize the formation of dendrite growth during the charging/discharging process of lithium batteries. It is reported that –CN groups in PAN could interact with –CO groups of liquid electrolytes such as propylene carbonate (PC), ethylene carbonate (EC), etc., as well as with lithium ions without losing the mechanical property [23]. However, PAN-based electrolytes show a decrease in ionic conductivity upon long storage due to the leakage of liquid electrolyte [24].

In our previous studies, we evaluated the electrochemical properties of PEs based on electrospun P(VdF-*co*-HFP) [1,2,6–9] and PAN [25]. The polymer electrolytes showed good electrochemical stability, high affinity to electrolyte solutions, desirable adhesion with electrode, and ionic conductivities in the range of 10^{-4} to 10^{-3} S cm^{-1} at room temperature. It is clear from our previous studies [1,2,6–9,25] and literatures that PAN [24] and P(VdF-*co*-HFP) [15] individually have beneficial characteristics as host polymers in PEs. P(VdF-*co*-HFP) could provide few important characteristics towards PEs which could not be derived from PAN or vice versa. Hence the polymer electrolytes based on the blend/composite P(VdF-*co*-HFP) and PAN may exploit the beneficial characteristics of both polymers.

Electrospinning is an alternative, efficient and simple method to prepare thin fibrous porous membranes with high level of porosity [1]. Moreover, the porous PAN membranes are very brittle for the reason that the interaction of adjacent cyanide groups increases the resistance of interior rotation of the main chain and decreases the flexibility of the membrane [26]. However, while electrospinning, highly polar nitrile groups in PAN hinder the alignment of macromolecular chains and hence make it flexible membrane with good mechanical strength. The process involved in the electrospinning could induce phase mixing between P(VdF-*co*-HFP) and PAN or avoid the phase separation.

In the present study we report the preparation and electrochemical characterization of polymer electrolytes based on electrospun blend and composite membranes of P(VdF-*co*-HFP) and PAN. The resultant membranes were converted into the polymer electrolytes by activating them with a liquid electrolyte, 1 M $LiPF_6$ in EC/DMC. The temperature dependent ionic conductivity and electrochemical properties of the PEs were evaluated in the process of testing their suitability for application as electrolytes in lithium batteries and the results were also compared.

2. Experimental

2.1. Preparation and characterization of electrospun membranes

PAN (Mw 150,000, Aldrich) and P(VdF-*co*-HFP) (Kynar Flex 2801, $M_w = 4.77 \times 10^5$, VdF/HFP ratio: 88/12, Elf Atochem) were vacuum dried at 60 °C for 6 h before use. The solvent N,N-dimethylformamide (DMF) (Aldrich) was used as received. Fibrous membranes were prepared by a typical electrospinning method at room temperature, as described in our previous publications [1,2]. For the preparation of the composite membranes a 14 wt% homogeneous solution of PAN or P(VdF-*co*-HFP) was prepared separately in DMF by mechanical stirring using high energy ball mill for 1 h at room temperature. The resulting solution was degassed for 15 min to get the bubble free clear solution. Sufficient amount of the polymer solution was alternatively supplied to a steel needle of bore size

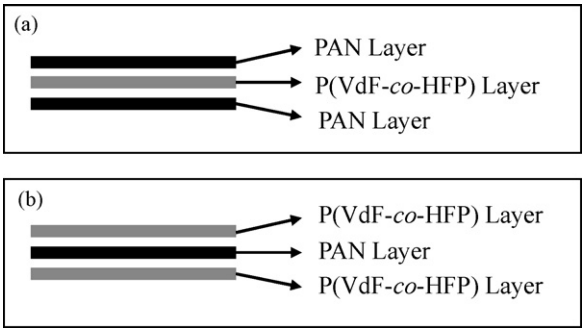

Fig. 1. Schematic representation of electrospun P(VdF-*co*-HFP)/PAN composite membranes: (a) PE-LM1 and (b) PE-LM2.

0.5 mm through a capillary using a syringe infusion/withdrawal pump (KD Scientific, Model 210). High electric voltage (18 kV) was applied to polymer solution by clamping the electrode of the power supply at the tip of the steel needle. A grounded, stainless-steel current collector in the shape of a drum covered with a thin aluminum foil, rotating at 150 rpm was used as the target for collecting fibers in the form of layer-by-layer structured composite membranes. Instead of assembling separate layers of the membranes, in the present work we adopted the continuous electrospinning, in which both the solutions are continuously fed to the tip of the needle one-by-one. Therefore, the resultant membranes have good adhesion between the layers. In the tailor-made composite membranes thickness of the each layer was carefully controlled during the electrospinning. The upper and lower layers have about 25 μm and the middle layer has about 50 μm thicknesses.

For preparing the membrane of polymer blend, 14 wt% solution of the polymers PAN and P(VdF-*co*-HFP) in the weight ratio of 50:50 was prepared in DMF using high energy ball mill and the resultant homogenous solution was electrospun. The essential electrospinning parameters were as follows: applied voltage 18 kV, distance between the tip of the spinneret and collector 20 cm, needle size 0.5 mm, solution feed rate 0.1 mL min^{-1} and collector drum rotation speed 150 rpm. Electrospun membranes of average thickness 100 μm were collected and dried for 6 h at room temperature on the drum for keeping the membrane in the stretched state to prevent the shrinking of fibers and then vacuum dried at 60 °C for 12 h before further use. These membranes were designated as PE-LM1 {PAN-P(VdF-*co*-HFP)-PAN layer-by-layer membrane}, PE-LM2 {P(VdF-*co*-HFP)-PAN-P(VdF-*co*-HFP) layer-by-layer membrane}, and PE-BM {PAN-P(VdF-*co*-HFP) blend membrane}to highlight their respective composition. The schematic representation of PE-LM1 and PE-LM2 is depicted in Fig. 1.

The surface morphology of the membrane was investigated with a high resolution field emission scanning electron microscope (SEM-JEOL JSM 5600). The average fiber diameter (AFD) was determined from the micrographs taken at high magnifications and about 250 fibers were investigated. The porosity (P) was determined by the n-butanol uptake method [1].

2.2. Preparation of PEs based on electrospun fibrous membranes

PEs were prepared by loading the circular membrane of about 2 cm^2 area for 1 h with 1 M lithium hexafluorophosphate ($LiPF_6$) in ethylene carbonate (EC)/dimethyl carbonate (DMC) (1:1, v/v) under an argon atmosphere in a glove box ($H_2O < 10$ ppm) at room temperature. The lithium salts and organic solvents were supplied by Samsung Cheil Industries Inc. $LiPF_6$ salt in mixed carbonate solvents (EC/DMC) was selected for the study because this electrolyte is generally employed in commercial lithium ion batteries.

2.3. Electrochemical measurements

Electrolyte uptake by the membrane was determined by soaking a circular piece of the membrane (diameter 1.5 cm) in electrolyte solution as reported elsewhere [1]. The weight of the wetted membrane was determined at different soaking intervals, taking care to remove the excess electrolyte remaining on the surface of the membrane by wiping softly with a tissue paper. The ionic conductivities of the PEs, over the temperature range −10 to 80 °C, were measured by the AC impedance analysis using stainless-steel (SS) Swagelok cells with an IM6 frequency analyzer. The measurements were performed over the frequency range of 100 mHz to 2 MHz at an amplitude of 20 mV. The electrochemical stability was determined by linear sweep voltammetry (LSV) of Li/PE/SS cells at a scan rate of 1 mV s^{-1} over the range of 2–6 V at 25 °C. The time dependent interfacial resistance (R_f) between the PE and lithium metal electrode was measured by the impedance response of Li/PE/Li cells over the frequency range 100 mHz to 2 MHz at an amplitude of 20 mV. The prototype lithium coin cells of 23 mm diameter was fabricated by sandwiching the fibrous membrane soaked in 1M $LiPF_6$ in EC/DMC (1:1, v/v) between a lithium metal anode (300 μm thickness, Cyprus Foote Mineral Co.) and lithium iron phosphate ($LiFePO_4$) cathode. The carbon-coated $LiFePO_4$ cathode active material was made in-house by mechanical activation followed by heat treatment at high temperature [27]. The cathode was prepared as its blend with conductive carbon and PVdF binder at a ratio of 80:10:10 by weight. The ingredients were mixed together in N-methylpyrrolidone (NMP) solvent to get homogeneous slurry which was cast on aluminum foil and dried under vacuum at 80 °C for 24 h to get the film of ∼23 μm thickness. The charge–discharge and cycling tests were conducted in an automatic galvanostatic charge–discharge unit, WBCS3000 battery cycler (WonA Tech., Co.), between 2.5 and 4.0 V at room temperature. The experiments were run at a current density rate of 0.1 C.

3. Results and discussion

3.1. Morphological characterization of electrospun membranes

The schematic representation of tailor-made composite membranes of P(VdF-*co*-HFP) and PAN is illustrated in Fig. 1. There are three layers in the composite membranes. The top and bottom layers are made of same polymer and the middle one is with second polymer. Both the top and bottom layers have about 25 μm and the middle layer has about 50 μm thickness. The membranes are prepared by the continuous electrospinning, in which the polymer solution was continuously fed to the tip of the needle one-by-one. The continuous electrospinning will make tailor-made composite membrane with good adhesion between the layers via physical crosslinking. By this method it is easy to tailor well-architected membranes having multi-layers with different polymers such as PMMA, PVAc, PEO, etc.

Fig. 2 shows SEM images of electrospun fibrous membranes depicting the morphological variation between the blend and composite membranes of P(VdF-*co*-HFP) and PAN. From the SEM images it is clear the membranes have a three-dimensional network structure composed of fully interconnected pores made up of ultrafine fibers with bead free morphology. This indicates that dry fibers are deposited by rapid evaporation of the solvent during electrospinning. The AFD of the membranes obtained under the studied conditions are 320 < 470 < 490 nm, respectively, for the membranes of PE-LM1, PE-LM2, and PE-BM. The difference in AFD is attributed to the difference in viscosity of the polymer solution and its rheological properties. The higher solution viscosity that leads to the ejection of larger drops from the needle forms larger fibers on deposition. Uniform membrane morphology with very narrow range of fiber diameter and AFD was obtained. From SEM images it can be seen that the interlaying of the fibers generates the highly porous fibrous structure for the electrospun membranes, which arises due to the processing parameters employed. The amount of DMF that remains on the surface of the fiber after electrospinning can partially dissolve and make it amorphous.

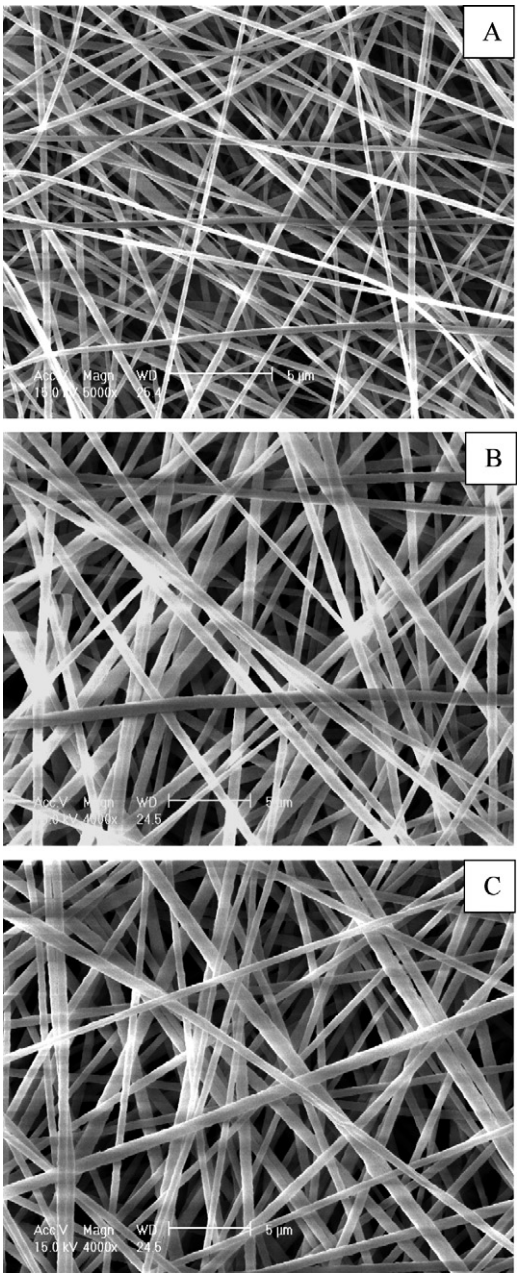

Fig. 2. SEM images of electrospun P(VdF-*co*-HFP)/PAN blend/composite membranes: (A) PAN, (B) P(VdF-*co*-HFP) and (C) 50:50 blend of P(VdF-*co*-HFP)/PAN.

The interlaying of fibers generates porous structure in the electrospun membranes. The porosity of the membrane varies in a narrow range of 82–85%, in the order of PE-LM2 < PE-LM1 < PE-BM. The difference in porosity is attributed to the three-dimensional packing structure of the membrane depending on the polarity and rheological properties of the polymer solutions. It is considered that the more porous network in the latter resulted from the loose packing of fibers in the layers of the membranes due to the synergy effect of both viscosity and phase separation property of the

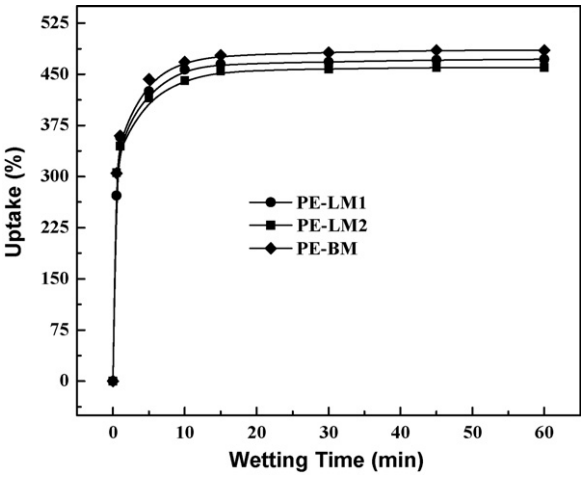

Fig. 3. Electrolyte uptake (%) of electrospun P(VdF-*co*-HFP)/PAN blend/composite membranes (1 M $LiPF_6$ in EC/DMC, 1:1, v/v).

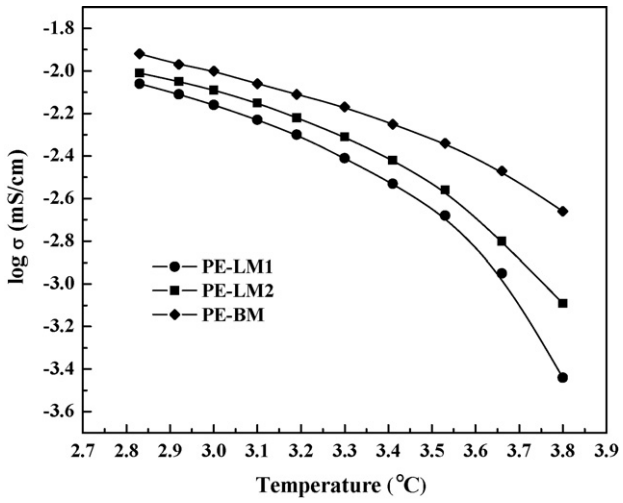

Fig. 4. Effect of temperature on ionic conductivity of polymer electrolytes based on electrospun P(VdF-*co*-HFP)/PAN blend/composite membranes (100 mHz to 2 MHz at an amplitude of 20 mV).

solution. The high porosity of the membranes was also reflected in their high electrolyte uptake of electrolyte solution with 460, 472, and 485% obtained for the membranes PE-LM2, PE-LM1, and PE-BM respectively. It is found that electrolyte uptake is higher for the membrane having higher porosity. In other words, the electrolyte uptake and ionic conductivity increase with porosity. Fig. 3 presents the comparison of electrolyte uptake (1 M $LiPF_6$ in EC/DMC) of the membranes. The fully interconnected pore structure of these membranes helps fast liquid penetration into the membrane, and hence the uptake process gets stabilized within a span of only 10 min. The absorption of the large quantities of liquid electrolyte by the membranes results from both the high porosity of the membranes and the partial gelation of the membranes. The gelation of the membranes is attributed to its affinity for electrolyte solution, which results from the polar functional groups in the polymer chains [24].

3.2. Ionic conductivity

The temperature dependent ionic conductivities of the PEs were studied at different temperatures by the AC impedance method. The PEs under the study comprise a solid polymer fiber phase, a partially swollen amorphous fiber phase, and a liquid electrolyte phase encapsulated in the pores of the membrane [28,29]. Two ion conduction paths have been postulated for porous-membrane based PEs: one is high conduction path through the liquid electrolyte phase and the other is slow conduction path through the swollen polymer phase [28,30]. From the impedance data, the ionic conductivity values of 3.9×10^{-3}, 4.9×10^{-3} and 6.5×10^{-3} S cm^{-1} were obtained at 25 °C, respectively, for PE-LM1, PE-LM2 and PE-BM. It is observed that the ionic conductivity of PE based on blend membrane is 1.3–1.7 times greater than that of composite membranes. The difference in conductivity is probably due to the difference in porosity and electrolyte uptake of the membranes. It is found that the order of porosity value and ionic conductivity is in the order of PE-LM1 < PE-LM2 < PE-BM. The ionic conductivities of the PEs based on electrospun PAN or P(VdF-*co*-HFP) membranes are lower than the composite/blend membranes of PAN and P(VdF-*co*-HFP). The ionic conductivities of the PEs at 25 °C were 4.2×10^{-3} (AFD 1.2 μm) [2] and 2.31×10^{-3} S cm^{-1} (AFD 350 nm), respectively, for P(VdF-*co*-HFP) and PAN. 1 M $LiPF_6$ in EC/DMC is reported to have an ionic conductivity of 10.7×10^{-3} S cm^{-1} at 25 °C [31]. The ionic conductivities of the PEs based on electrospun membranes were lower than that of the liquid electrolyte. The PE-BM showed the ionic conductivity ~39% lower than that of liquid electrolyte 1 M $LiPF_6$ in EC/DMC at 25 °C. However, it is 15–25% (calculated with respect to liquid electrolyte) higher than the ionic conductivities of polymer electrolytes PE-LM1 and PE-LM2 at 25 °C. This is due to the slow ion conduction path in the swollen submicron fiber phase and the poor tortuosity in the pore structure. A smooth and linear enhancement in conductivity with temperature was observed for all PEs examined here. In polymer complex systems, the change of conductivity with temperature may be due to the segmental motion of the polymer chains leading to increase in free volume in the system, which will provide an easy pathway for the transitional motion of the ions. The segmental motion also permits the ions to hop from one site to another. As the temperature increases, both the segmental motion and transitional ionic motion in the system will be increased due to the high activation energy and it will increase the ionic conductivity of the PEs [32,33]. However, the variation of conductivity with temperature is minimal beyond the temperature 50 °C for all the PEs, this is because the electrolyte used (EC or DMC) has the melting point below 40 °C and forms a low viscous medium for the ion transportation beyond the melting temperature of the electrolyte. Both composite or blend polymer electrolytes reported here exhibited higher ionic conductivities above 3.9×10^{-3} S cm^{-1} at 25 °C, which makes them suitable for the use in lithium polymer batteries at room temperature.

Fig. 4 shows the Arrhenius plot of ionic conductivity of the PEs in the temperature range of −10 to 80 °C. The conductivity of the membranes was sharply decreased below 0 °C, due to the freezing property of carbonate solvents in the electrolyte solutions. A smooth and linear enhancement in ionic conductivity was observed with an increase in temperature from −10 to 80 °C. The difference in ionic conductivities between −10 and 80 °C is the lowest for PE-BM. It was observed that within the temperature range −10 to 80 °C the Arrhenius plots are slightly curved, so that the activation energy for ionic conduction E_a can be obtained using the Vogel–Tamman–Fulcher (VTF) model $\{\sigma = \sigma_0 T^{-1/2} \exp[-E_a/R(T - T_0)]\}$ instead of the simple Arrhenius model $[\sigma = \sigma_0 \exp(-E_a/RT)]$ used for the treatment of the linear Arrhenius plots. From the parallel curves of all the samples it can be suggested that given the low difference in the activation energies and porosity of different samples, the variation of average pore size does not influence the activation energy for ionic conduction.

3.3. Electrochemical properties

The electrochemical stability of polymer electrolytes by LSV is presented in Fig. 5. Although the ionic conduction is occur-

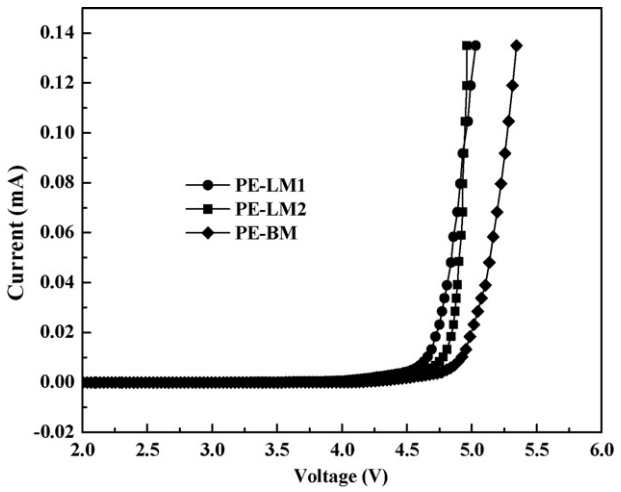

Fig. 5. Anodic stability by LSV of polymer electrolytes based on electrospun P(VdF-*co*-HFP)/PAN blend/composite membranes (Li/PE/SS cells, 1 mV s^{-1}, 2–5.5 V).

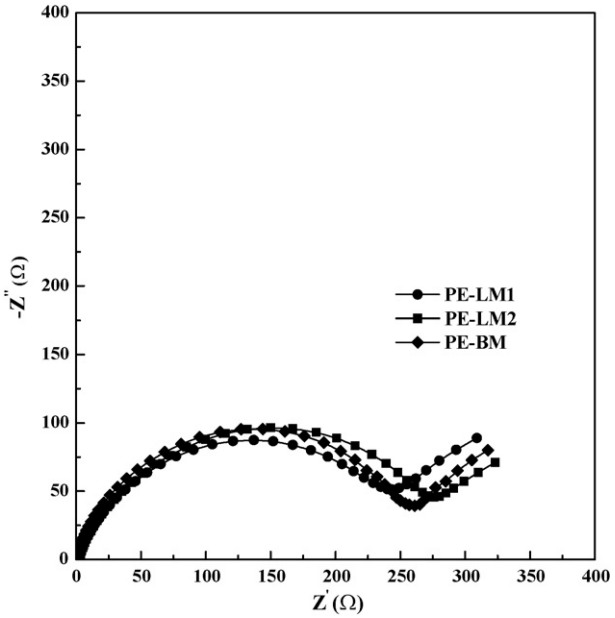

Fig. 6. Initial AC impedance behaviors of polymer electrolytes based on electrospun P(VdF-*co*-HFP)/PAN blend/composite membranes (Li/PE/Li cells, frequency range 100 mHz to 2 MHz).

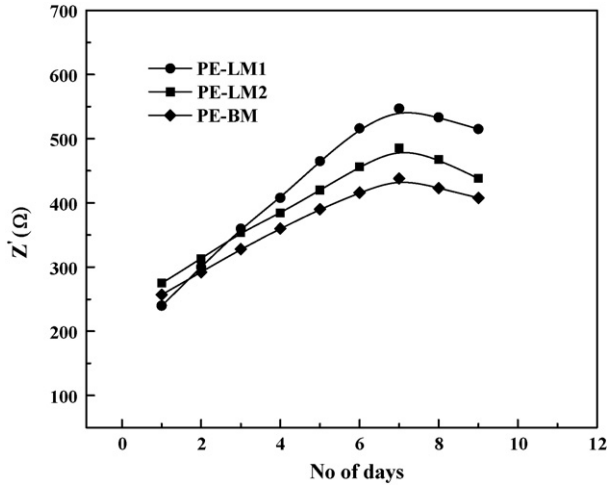

Fig. 7. Variation of interfacial resistance of polymer electrolytes based on electrospun P(VdF-*co*-HFP)/PAN blend/composite membranes with storage time (Li/PE/Li cells, frequency range 100 mHz to 2 MHz).

ring mainly through the entrapped liquid electrolyte in the porous structure, the partially swollen fibrous matrix with large surface area contributes significantly to the enhancement of the electrochemical stability of the PE. All the PEs based on electrospun membrane studied here exhibit an anodic stability greater than 4.6 V versus Li/Li^+. The high anodic stability is caused by the excellent affinity to the carbonate based liquid electrolyte solution which will partially dissolve the fibers. Therefore, the swollen phase of the membrane probably includes the complex compounds such as associated –CN–Li^+ or VdF–Li^+ groups, the associated –CO–Li^+ group and the associated –CN–Li^+–OC– group or VdF–Li^+–OC– group. This complex formation with lithium ion and dipole–dipole interaction between the CO group of the carbonate molecules and VdF groups of P(VdF-*co*-HFP) or –CN pendent groups of the PAN greatly enhance the electrochemical stability of the resulting polymer electrolytes. The large and fully interconnected pores, high porosity, higher specific surface area, uniform morphology of membranes and thinner fiber diameter also influence the enhancement of the electrochemical stability of these PEs. The order of electrochemical stability is 4.6 < 4.7 < 4.9 V for PE-LM1, PE-LM2, and PE-BM, respectively. The earlier studies also have been reported on high electrochemical stability for PEs based on electrospun PAN [34], PVdF [29,35] and P(VdF-*co*-HFP) [1,2,30]. An anodic stability of about 4.5 V has earlier been reported for P(VdF-*co*-HFP) based polymer electrolyte [1]. The high electrochemical stability for PE-BM than PE-LMs may be due to the synergy effect of P(VdF-*co*-HFP) and PAN in the blend membrane. The high anodic stability of these polymer electrolytes should render them potentially compatible with the high voltage cathode materials like $LiCoO_2$ and $LiMn_2O_4$ commonly used in lithium ion batteries.

Compatibility of the electrolyte with lithium metal anode is an important factor that determines the cycle performance of lithium cells. The initial impedance behaviors of PEs based on electrospun P(VdF-*co*-HFP)/PAN blend/composite membranes are presented in Fig. 6. The impedance spectra are in the form of semi circles typical of electrolytes with contribution from bulk electrolyte resistance (R_b) and electrode/electrolyte interfacial resistance (R_f). The real axis intercept at the high frequency end of the spectra denotes the R_b of the polymer electrolyte and is very low (2.3–3.6 Ω). There was no appreciable change in R_b with storage time up to 9 days. This behavior is indicative of a good retention of the ionic conductivity of the PE consisting of a swollen fibrous structure. The data show that the initial R_f values vary in the range of 240–275 Ω for the PEs.

The variation of interfacial resistance with storage time is shown in Fig. 7. It is found that the interfacial resistance increases with storage time to reach a maximum and then starts to decrease. The initial increase in R_f with time is inevitable in lithium metal batteries as it indicates the formation and growth of the passivation layer on lithium surface by a reaction with the electrolyte components, impeding the passage of ions. The formation of passivation layer prevents further reaction of the electrolyte with lithium, helps to enhance the cathodic limit of the electrolyte, and thus improves cycling properties. It is found that the R_f initially increased during 7 days, and decreased thereafter. The initial R_f values were 240, 257, and 275 Ω for PE-LM1, PE-BM, and PE-LM2, respectively. After 7 days, the R_f values increased from 70 to 128% compared to the initial R_f values. The maximum increase in R_f with time is observed for PE-LM1 (128%) and the least with PE-BM (70%) after 7 days. It is found that the interfacial resistance is comparatively quite low and increases slowly upon storage time. The favorable interfacial

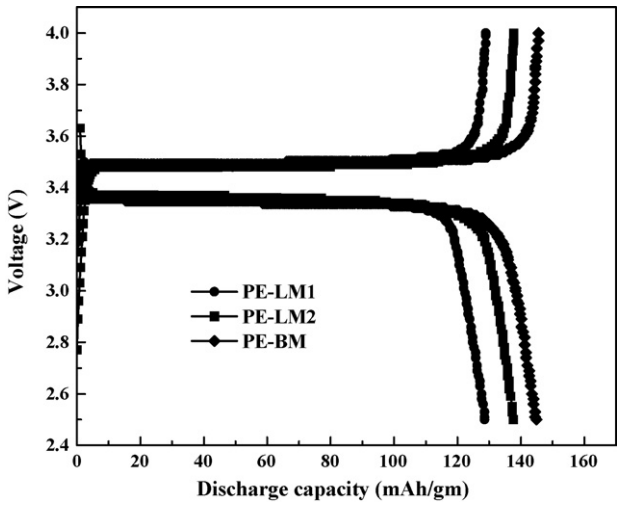

Fig. 8. Initial charge–discharge properties of Li/PE/$LiFePO_4$ cells with polymer electrolytes based on electrospun P(VdF-*co*-HFP)/PAN blend/composite membranes (25 °C, 0.1 C-rate, 2.5–4.0 V).

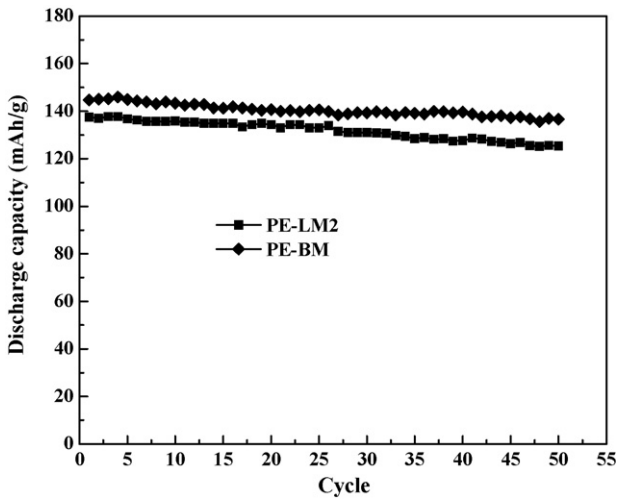

Fig. 9. Cycle properties of Li/PE/$LiFePO_4$ cells with polymer electrolytes based on electrospun P(VdF-*co*-HFP)/PAN blend/composite membranes (25 °C, 0.1 C-rate, 2.5–4.0 V).

properties reflect a good electrode behavior with the PEs making very promising candidate for safe, reliable and long lasting lithium batteries.

3.4. Evaluation in Li/$LiFePO_4$ cell

The polymer electrolytes based on composite/blend membranes have been evaluated for charge/discharge performance in Li/$LiFePO_4$ cells at room temperature. $LiFePO_4$ has attracted much attention as the next generation cathode material. It has a high theoretical capacity of 170 mAh g^{-1}, an operating potential of 3.4 V, and excellent cycling properties. Compared with the transition metal oxides presently used as cathode materials in lithium ion batteries, $LiFePO_4$ is non-toxic, cheaper and easy to prepare. The first cycle charge–discharge properties at a current density corresponding to 0.1 C-rate are compared in Fig. 8. Relatively high cathode utilization corresponding to 77–85% of theoretical capacity was achieved.

The cell based on the polymer electrolyte with PE-BM delivers initial charge and discharge capacities of 145 mAh g^{-1}, which correspond to 85% utilization of the active material. The performance of the cell with polymer electrolyte containing composite membranes are lower, with a discharge capacity of 130 and 138 mAh g^{-1} was obtained for PE-LM1 and PE-LM2 respectively, which is 19–23% lower than the theoretical capacity.

The difference in discharge capacity is probably due to the difference in the utilization of active material. The PE-BM contains the largest amount of liquid electrolyte among them, and hence much liquid electrolyte can diffuse from the polymer electrolyte to the composite cathode, which leads to higher utilization of the active material. The difference in ionic conductivity of the PEs also may affect the discharge property. It was observed that the cell with PE based on electrospun membrane of P(VdF-*co*-HFP) [2] and PAN [25] showed 145 and 148 mAh g^{-1}, respectively.

The cycle performance of the cell with PE-LM2 and PE-BM up to 50 cycles was studied and is shown in Fig. 9. After 50 cycles the cell with PE-BM retains 94% of initial discharge capacity which corresponds to 81% of the theoretical capacity, while the cell with PE-LM2 delivers only 73.5% of the theoretical capacity. The discharge capacity fade of 0.14 and 0.26 mAh g^{-1} per cycle was observed after the 50th cycle (over initial capacity) for the cells with PE-BM and PE-LM2, respectively. In our earlier study [36], an evaluation was made of the performance of Li/$LiFePO_4$ cells under similar conditions using the liquid electrolyte of 1 M $LiPF_6$ in EC/DMC. It is seen that the performance of PEs based on electrospun P(VdF-*co*-HFP)/PAN blend/composite membranes is as good as the liquid electrolyte. The capacity fade is also comparable for both the PE and liquid electrolyte. The good cycle property of the cell can be attributed to enabling free passage of ions between electrodes and good compatibility between the electrolyte and electrode, especially with lithium metal. This evaluation demonstrates the suitability of PEs based on electrospun P(VdF-*co*-HFP)/PAN blend/composite membranes for lithium battery applications.

4. Conclusions

PEs based on fibrous P(VdF-*co*-HFP)/PAN blend/composite membranes were prepared by electrospinning of the polymer solution in DMF. Fibrous membranes with uniform morphology and AFD of 320–490 nm have been prepared under the optimized condition of 14 wt% solution in DMF at 18 KV. The PEs were prepared by activating the membranes with 1 M $LiPF_6$ in EC/DMC. All the PEs exhibited a high ionic conductivity in the range of 10^{-3} S cm^{-1} at 25 °C. The PEs have good electrochemical stability >4.6 V versus Li/Li^+, and have a stable R_f value on lithium metal. Compared to the PEs based on composite membranes, blend membranes showed higher electrolyte uptake, higher ionic conductivity, stable interfacial resistance, higher electrochemical stability window and cycle performance. The resulting good discharge capacity and cycle performance indicate that PEs based on electrospun blend/composite membranes are suitable for application in safe, reliable and long lasting lithium batteries. P(VdF-*co*-HFP)/PAN blend/composite polymer electrolytes in lithium batteries are superior in performance to the membranes of individual polymers PAN and P(VdF-*co*-HFP). Thus, the present methodology of the preparation of blend/composite membranes using electrospinning can be extended for the preparation of wide range of other tailor-made polymer blend/composites membranes.

Acknowledgements

This research was supported by Basic Science Research Program Through the National Research Foundation (NRF) funded by the Ministry of Education, Science and Technology (KRF-2008-313-D00299) and also by the Ministry of Knowledge Economy (MKE)

and Korea Industrial Technology Foundation (KOTEF) through the Human Resource Training Project for Regional Innovation.

References

[1] P. Raghavan, J.W. Choi, J.H. Ahn, G. Cheruvally, G.S. Chauhan, H.J. Ahn, A. Nah, J. Power Sources 184 (2008) 437.
[2] P. Raghavan, X. Zhao, J.K. Kim, J. Manuel, G.S. Chauhan, J.H. Ahn, C. Nah, Electrochim. Acta 54 (2008) 228.
[3] C.Y. Chiang, M.J. Reddy, P.P. Chu, Solid State Ionics 175 (2004) 631.
[4] Y.J. Wang, D. Kim, Electrochim. Acta 52 (2007) 3181.
[5] V. Gentili, S. Panero, P. Reale, B. Scrosati, J. Power Sources 170 (2007) 185.
[6] P. Raghavan, X. Zhao, J. Manuel, G.S. Chauhan, J.H. Ahn, H.S. Ryu, H.J. Ahn, K.W. Kim, C. Nah, Electrochim. Acta doi:10.1016/j.electacta.2009.05.025.
[7] X. Li, G. Cheruvally, J.K. Kim, J.W. Choi, J.H. Ahn, K.W. Kim, H.J. Ahn, J. Power Sources 167 (2007) 491.
[8] G. Cheruvally, J.K. Kim, J.W. Choi, J.H. Ahn, Y.J. Shin, J. Manuel, P. Raghavan, K.W. Kim, H.J. Ahn, D.S. Choi, C.E. Song, J. Power Sources 172 (2007) 863.
[9] J.K. Kim, G. Cheruvally, X. Li, J.H. Ahn, K.W. Kim, H.J. Ahn, J. Power Sources 178 (2008) 815.
[10] N.T.K. Sundaram, A. Subramania, Electrochim. Acta 52 (2007) 4987.
[11] G. Jiang, S. Maeda, H. Yang, Y. Saito, S. Tanase, T. Sakai, J. Power Sources 141 (2005) 143.
[12] A.I. Gopalan, P. Santhosh, K.M. Manesh, J.H. Nho, S.H. Kim, C.G. Hwang, K.P. Lee, J. Membr. Sci. 325 (2008) 683.
[13] Y.H. Liao, D.Y. Zhou, M.M. Rao, W.S. Li, Z.P. Cai, Y. Liand, C.L. Tan, J. Power Sources 189 (2009) 139.
[14] J.W. Choi, G. Cheruvally, Y.H. Kim, J.K. Kim, J. Manuel, P. Raghavan, J.H. Ahn, K.W. Kim, H.J. Ahn, D.S. Choi, C.E. Song, Solid State Ionics 178 (2007) 1235.
[15] A.D. Pasquier, F. Disma, T. Bowmer, A.S. Gozdz, G. Amatucci, M. Tarascon, J. Electrochem. Soc. 145 (1988) 472.
[16] Elf-Atochem's technical brochure, Kynar and Kynar Flex PVdF.
[17] F. Boudin, X. Andrieu, C. Jehoulet, I.I. Olsen, J. Power Sources 81–82 (1999) 804.
[18] S. Abbrent, J. Pletstil, D. Hlavata, J. Lindgren, J. Tegenfeldt, A. Wendsjo, Polymer 42 (2001) 1407.
[19] D.J. Lin, C.L. Chang, C.K. Lee, L.P. Cheng, Eur. Polym. J. 42 (2006) 2407.
[20] I. Nicotera, L. Coppola, C. Oliviero, M. Castriota, E. Cazzanelli, Solid State Ionics 177 (2006) 581.
[21] B. Huang, Z. Wang, L. Chen, R. Xue, F. Wang, Solid State Ionics 91 (1996) 279.
[22] H. Tsutsumi, A. Matsuo, K. Takase, S. Doi, A. Hisanaga, K. Onimura, T. Oishi, J. Power Sources 90 (2000) 33.
[23] K.M. Abraham, M. Alamgir, J. Electrochem. Soc. 137 (1990) 1657.
[24] H.S. Min, J.M. Ko, D.W. Kim, J. Power Sources 119–121 (2003) 469.
[25] P. Raghavan, J. Manuel, C. Shin, M.Y. Heo, J.H. Ahn, to be published.
[26] G. Wu, H.Y. Yang, H.Z. Chen, F. Yuan, L.G. Yang, M. Wang, R.J. Fu, Mater. Chem. Phys. 104 (2007) 284.
[27] J.K. Kim, J.W. Choi, G. Chereuvally, J.U. Kim, J.H. Ahn, K.W. Kim, H.J. Ahn, Mater. Lett. 61 (2007) 3822.
[28] J. Saunier, F. Alloin, J.Y. Sanchez, G. Caillon, J. Power Sources 119–121 (2003) 454.
[29] S.W. Choi, S.M. Jo, W.S. Lee, Y.R. Kim, Adv. Mater. 15 (2003) 2027.
[30] J.R. Kim, S.W. Choi, S.M. Jo, W.S. Lee, B.C. Kim, J. Electrochem. Soc. 152 (2005) A295.
[31] M. Schmidt, U. Heider, A. Kuehner, R. Oesten, M. Jungnitz, N. Iganat'ev, P. Sartori, J. Power Sources 97–98 (2001) 557.
[32] S.D. Druger, A. Nitzam, M.A. Ratner, J. Chem. Phys. 79 (1983) 3133.
[33] S.D. Druger, A. Nitzam, M.A. Ratner, Phys. Rev. B31 (1985) 39.
[34] S.W. Choi, J.R. Kim, S.M. Jo, W.S. Lee, Y.R. Kim, J. Electrochem. Soc. 152 (2005) A989.
[35] J.R. Kim, S.W. Choi, S.M. Jo, W.S. Lee, B.C. Kim, Electrochim. Acta 50 (2004) 69.
[36] J.K. Kim, G. Cheruvally, J.W. Choi, J.U. Kim, J.H. Ahn, G.B. Cho, K.W. Kim, H.J. Ahn, J. Power Sources 166 (2007) 211.